Spin transfer by nonuniform current injection into a nanomagnet

O. Ozatay,[a] N. C. Emley, P. M. Braganca, A. G. F. Garcia, G. D. Fuchs, I. N. Krivorotov, R. A. Buhrman, and D. C. Ralph
Cornell University, Ithaca, New York 14853-2501

(Received 21 January 2006; accepted 4 April 2006; published online 18 May 2006)

We have used nanofabrication techniques to incorporate an ~20–30 nm diameter nanoaperture within a 150×250 nm^2 elliptical magnetic multilayer to enable the localized injection of spin-polarized currents into a thin film nanomagnet. This results in very low spin transfer currents being required for at least partial nanomagnet reversal as well as for onset of dynamic precession. Micromagnetic simulations using Landau-Liftshitz-Gilbert equation with a spin-torque term indicate that reversal occurs via domain nucleation at the injection site followed by domain wall propagation away from the aperture, with the nanomagnet ending in one of several different states depending upon the current amplitude. © *2006 American Institute of Physics*. [DOI: 10.1063/1.2206683]

A sufficiently large spin-polarized current passing through a magnetic multilayer can induce microwave frequency precession or switching between stable states via application of a spin-transfer torque, as originally predicted by Slonczewski[1] and Berger.[2] This mechanism has potential applications as an alternative to Oersted field switching in magnetic random access memory (MRAM), as a current-controlled nanoscale microwave oscillator, and in programmable logic. The potential technological applicability of the effect has triggered an intensive effort to optimize the device geometry and choice of materials to obtain reduction in switching currents.[3] Some current-perpendicular-to-plane (CPP) geometries where spin transfer induced excitations have been observed include nanopillars,[4–7] nanowires,[8] and nanocontacts to continuous films.[9–11] Although they require longer and more difficult fabrication procedures, nanopillars and nanowires do show at least an order of magnitude reduction in threshold currents for spin-transfer excitation compared to nanocontacts, due to the absence of coupling to an extended film. However, both theoretically[12] and experimentally,[13] it has been shown that nanocontacts act as ideal sites for domain wall nucleation, and spin-transfer-triggered domain wall motion makes domain wall switching a viable option for a magnetic bit.

In this work we have developed a fabrication technique to insert a nanoaperture inside a nanopillar. This geometry allows the concentrated, local injection of a spin-polarized current into a nanomagnet, as well as the local probing of the result of the spin transfer effect via the spin-valve magnetoresistance effect.

We start with a Permalloy (Py)/Cu stack capped with a 7 nm thick Al_2O_3 insulator. A 20–30 nm diameter nanohole is defined on an electron-beam resist layer using aligned e-beam lithography and then transferred halfway into the insulating layer via ion milling. The residual resist is etched away by O_2 plasma reactive ion etching. The device is transferred into a dc magnetron sputtering system equipped with an ion mill with a base pressure of 5×10^{-8} Torr. The hole etch in the oxide layer is completed by ion milling which stops at the Py layer. This milling step is followed by an *in situ* deposition of the rest of the metallic stack. After this point the device goes through a standard aligned nanopillar fabrication process with an alignment accuracy of 10 nm. Figure 1(a) shows a scanning electron micrograph (SEM) of a 150×250 nm^2 elliptical nanopillar and an atomic force microscope (AFM) image of a nanohole defined on a resist layer. The final device structure is displayed in Fig. 1(b). It consists of a 20 nm Py/8 nm Cu/5 nm Py spin valve with a 20–30 nm diameter nanohole located between the spacer layer and the thin, "free" Py layer.

All measurements were taken at 4.2 K to ensure thermal stability of the relatively low aspect ratio free layer nanomagnet. We examined 15 samples, whose resistances varied between 10 and 15 Ω, as compared to 3–5 Ω resistance exhibited by 100×200 nm^2 elliptical spin-valve nanopillars with the same magnetic multilayer structure but without the oxide aperture. This indicates that the device resistance in the former case is indeed determined by the aperture size rather than by the pillar area.

The minor hysteresis loop of the free layer for a sample with a nanoaperture is shown in the inset to Fig. 2(a). This was generated by fixing the thick Py layer magnetization by applying a large external field H_{ex} and then sweeping H_{ex} back and forth about the value that cancels the average dipole field on the free layer arising from the magnetic edge

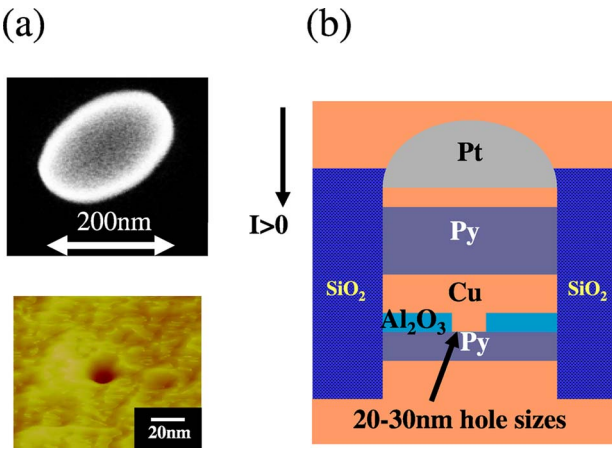

FIG. 1. (Color online) (a) Top—SEM image of a 150×250 nm^2 elliptical nanopillar. Bottom—AFM image of a 20 nm hole etched into the resist layer. (b) A schematic drawing of the final pillar device.

[a]Electronic mail: oo24@cornell.edu

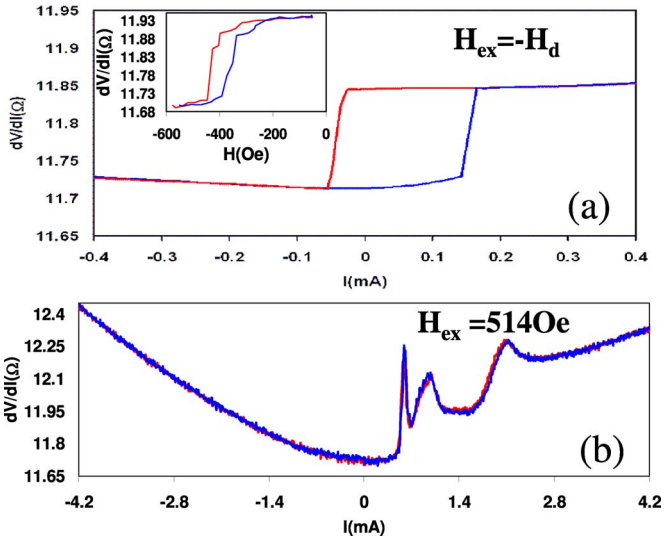

FIG. 2. (Color online) (a) A typical dV/dI vs I scan taken at 4.2 K with an applied field canceling the average dipolar field acting on the free layer from the fixed layer, displaying AP-to-P switching at −50 μA and P-to-AP switching at 180 μA. Inset: the magnetoresistance minor loop behavior of the free layer of the same nanopillar device shows a multiple step switching behavior attributable to domain wall pinning by defects induced at the contact region by the nanoaperture fabrication process. (b) A current scan of the same device taken at an applied field of ~500 Oe that displays peaks in the positive current branch that are generally indicative of the onset of persistent microwave dynamics within the free layer.

charges on the thicker "fixed" Py layer. Rather than exhibiting an abrupt transition, the minor loop displays steps, which are possibly due to the existence of defects in the free layer near the contact region introduced during ion milling of the nanoaperture. Nevertheless, the measured values of the dipolar field (H_d=375 Oe) and the free layer coercive field (H_c=40 Oe) are in reasonable agreement with a three dimensional (3D) micromagnetic simulation[14] of the field switching at zero temperature, which yields 340 Oe for H_d and 60 Oe for H_c. The small discrepancy between the simulation and the experimental values can be attributed to lithographic edge roughness of the nanopillar.

Figure 2(a) shows a resistance versus current scan of the same device taken with H_{ex} that cancels H_d. The measured spin-transfer switching currents, 180 μA for parallel (P) to antiparallel (AP) and −50 μA for AP to P, are much smaller than those of a 100×200 nm^2 pillar without the oxide aperture, 7.8 mA for P to AP and −4 mA for AP to P (not shown). The critical current densities for spin torque switching of the free layer at the aperture and for free layer switching in a pillar without the aperture are both $\sim1\times10^7$ A/cm^2. If, for comparison, the switching current for the nanoaperture device is distributed uniformly over the entire nanopillar cross-sectional area, this would be equivalent to a spin torque switching current density of $\sim4\times10^5$ A/cm^2, far lower than seen in any nonapertured nanopillar device. We do need to note that the total change in resistance does not correspond to the ΔR for full reversal as seen in the magnetoresistance minor loop. We tentatively explain this as due to the domain wall nucleated by a spin polarized current being pinned by a defect in the vicinity of the contact region. Evidence for distinct multistep spin-transfer switching has been occasionally seen in other samples. If such pinning occurs in the vicinity of the aperture, so as to be observable in the magnetoresistance but somewhat away from the location of the minimum contact area where the current density is lower, an increased critical current for reversal can be expected.

Figure 2(b) shows a resistance versus current scan of the same nanoaperture device taken with an applied field $H_{ex}>H_d$ which puts the free layer parallel to the fixed layer in the absence of a sufficiently large positive bias current. The peaks in dV/dI for positive currents indicate the onset of a dynamic precession regime within the free layer[5] at applied currents of less than 1 mA. This low onset current is consistent with the data in Fig. 2(a) that collectively point to a strong, highly localized spin torque at the aperture region of the free layer. Figure 2(b) also shows a substantial parabolic background in the dV/dI vs I curve, due to Joule heating. The asymmetry of this background with current direction is due to the Oersted field H_I generated by the current flowing through the aperture which results in the free layer taking the form of a C state[15,16] bending at the contact region (see the discussion on simulations in the next paragraph). For negative bias currents this leads to an increasing misalignment with bias between the otherwise parallel fixed and free layer magnetizations resulting in an increased resistance that adds to the parabolic background caused by Joule heating. For positive bias currents the contribution to the resistance is negative in the antiparallel case which exists above the switching current level as H_I bending acts to close the angle in between the magnetizations of the two layers.

This effect of H_I on the micromagnetic state of the free layer is confirmed by zero temperature 3D micromagnetic simulations using OOMMF (Ref. 14) code, extended to include the Slonczewski torque term[18] that we performed to investigate the switching mechanism of our devices. H_I was modeled assuming a current flow at the center of the pillar through a wire whose radius is equal to the contact radius. A static, field-switching simulation was performed first to find the micromagnetic state of the free layer for the case of an applied field H_{ex} that cancels the average value of the dipolar field seen by the free layer. Under these conditions the simulation indicated that the free layer would be in a leaf state.[17] The augmented Landau-Liftshitz-Gilbert simulation was initialized to start with the free layer in this micromagnetic state. The simulated spin torque equation is in the form[3] $g(\theta)=[A\sin(\theta)]/[1+B\cos(\theta)]$, where A is the torque amplitude and is proportional to the current polarization P and B is the spin torque asymmetry parameter.

The simulation parameters were chosen as follows. The saturation magnetization of unpatterned Py multilayer films was measured to be 650 emu/cm^3 at 4.2 K. The current polarization at 4.2 K was calculated from the magnetoresistance behavior with a two channel Valet-Fert model[19] to be 0.54. We assumed that the polarization direction is misaligned from the easy axis of the free layer by 1° and that the exchange stiffness is 13×10^{-12} J/m. The Gilbert damping parameter was chosen to be 0.014, which is larger than the typical value for uniform Py thin films, but actually somewhat smaller than that deduced from Py nanopillar switching experiments.[3] The torque asymmetry parameter B was chosen to be 0.6. The simulation cell size in all directions was taken to be 2.5 nm.

Figure 3(a) shows the simulated evolution of magnetization reversal for AP-to-P switching at 0.5 mA applied current and with $H_{ex}=-H_d$. The spin-polarized current injection at this current amplitude causes a domain nucleation under the contact region. The domain wall near the contact is forced to

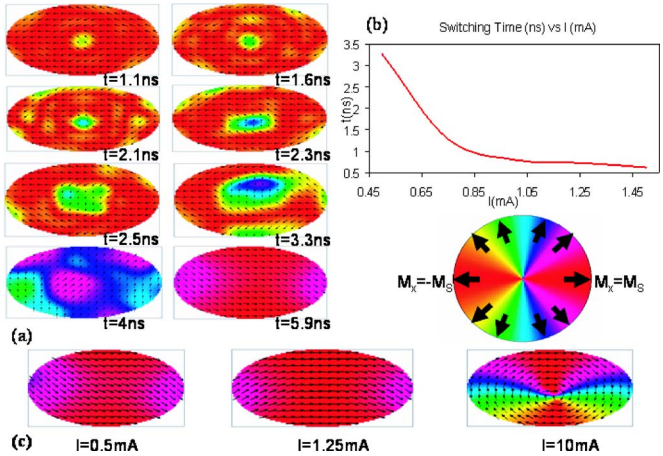

FIG. 3. (Color online) (a) A micromagnetic simulation of spin transfer switching from AP-to-P state of a nanomagnet subject to local current injection through a nanoaperture. In the simulation the highly localized spin torque nucleates a domain at the aperture. The resulting domain wall is pushed by current pressure via the magnetic balloon effect to interact with the device edges. Reversal is triggered when the domain underneath the contact touches the device edge. (b) A plot of simulated switching time vs applied current amplitude for AP-to-P switching. (c) The three possible micromagnetic configurations of the nanomagnet under the application of different pulse current amplitudes. The lowest switching current amplitude results in an *S* state. At higher amplitude a *C* state is the result, while a still higher pulse level results in a vortex state that is displaced from the aperture as long as the current pulse remains.

propagate into the nanomagnet via current pressure. The domain wall then expands as in the magnetic balloon effect[20] and interacts with the edge charges. The nanocontact acts as a source of domain walls, which are continuously pushed to apply a torque to the nanomagnet. Once the domain underneath the contact grows to be large enough to touch the device edges, magnetic reversal is triggered.

This domain wall mediated magnetization reversal has the disadvantage of being a slower reversal process than reversal by uniformly driven nanomagnet precession, especially in the presence of defects that act as domain wall pinning centers. Simulation results for the *free layer switching time* versus I are shown in Fig. 3(b). The simulations indicate that the reduction in switching speed can be compensated by applying current pulses of larger amplitude. However, the final micromagnetic configuration to which the device switches is affected by the amplitude of the applied current as shown in Fig. 3(c). When the applied current is low enough that H_I is negligible, the domain wall mediated reversal results in an *S* state. For somewhat higher current levels H_I results in the free layer magnetization ending in a *C* state, while for very large current levels this *C* state can even evolve into a vortex where the center of the vortex is displaced from the aperture due to the strong spin torque. When the current pulse is removed in the simulation, the different micromagnetic states persist, with the exception that the vortex that can be created at very high pulse levels moves to a position centered over the aperture.

In conclusion, we have fabricated elliptical Py/Cu nanopillar spin valves with a 20–30 nm diameter nanoaperture at the interface between the Cu spacer and the Py free layer. Low temperature spin transfer measurements yield very low absolute critical current levels for spin torque switching, with the required current density at the hole being comparable to the experimental values required for spin torque switching of the same size nanopillar with uniform injection. 3D micromagnetic simulations indicate that the reversal process is via the nucleation of a localized domain wall which then is driven across the free layer by the magnetic balloon effect. Thus this mechanism, especially in the absence of defect pinning, results in reduced switching currents. The data indicate that spin injection via a highly localized spin valve contact to a ferromagnetic line could be a much more efficient spin torque mechanism for initiating domain wall displacement than current injection across a domain wall.[21] However, this reduced switching current is accompanied by a slower free layer reversal rate. Faster switching can, of course, be obtained as indicated by the simulations by applying progressively larger amplitude current pulses.

The authors thank John Treichler of Cornell Nanoscale Science and Technology Facility for his expert help with high-resolution electron beam alignment. This work was supported by the Army Research Office MURI program in Spin Interactions and Spin Dynamics in Nanostructures and by NSF through the NSEC support of the Center for Nanoscale Systems and through use of the National Nanofabrication Infrastructure Network/Cornell Nanoscale Facility.

[1] J. C. Slonczewski, J. Magn. Magn. Mater. **159**, L1 (1996).
[2] L. Berger, J. Appl. Phys. **90**, 4632 (2001).
[3] P. M. Braganca, I. N. Krivorotov, O. Ozatay, A. G. F. Garcia, N. C. Emley, J. C. Sankey, D.C. Ralph, and R. A. Buhrman, Appl. Phys. Lett. **87**, 112507 (2005).
[4] J. A. Katine, F. J. Albert, R. A. Buhrman, E. B. Myers, and D. C. Ralph, Phys. Rev. Lett. **84**, 3149 (2000).
[5] S. I. Kiselev, J. C. Sankey, I. N. Krivorotov, N. C. Emley, R. J. Schoelkopf, R. A. Buhrman, and D. C. Ralph, Nature (London) **425**, 380 (2003).
[6] J. Z. Sun, J. Magn. Magn. Mater. **202**, 157 (1999).
[7] B. Ozyilmaz, A. D. Kent, D. Monsma, J. Z. Sun, M. J. Rooks, and R. H. Koch, Phys. Rev. Lett. **91**, 067203 (2003).
[8] J. E. Wegrowe, D. Kelly, Y. Jaccard, P. Guittienne, and J. P. Ansermet, Europhys. Lett. **45**, 626 (1999).
[9] E. B. Myers, D. C. Ralph, J. A. Katine, R. N. Louie, and R. A. Buhrman, Science **285**, 867 (1999).
[10] W. H. Rippard, M. R. Pufall, and T. J. Silva, Appl. Phys. Lett. **82**, 1260 (2003).
[11] M. Tsoi, A. G. M. Jansen, J. Bass, W. C. Chiang, M. Seek, V. Tsoi, and P. Wyder, Phys. Rev. Lett. **80**, 4281 (1998).
[12] P. Bruno, Phys. Rev. Lett. **83**, 2425 (1999).
[13] O. Ozatay, P. Chalsani, N. C. Emley, I. N. Krivorotov, and R. A. Buhrman, J. Appl. Phys. **95**, 7315 (2004).
[14] M. J. Donahue and D. G. Porter, 00MMF User's Guide, Version 1.0 Interagency Report NISTIR 6376, National Institute of Standards and Technology, Gaithersburg, 1999.
[15] M. Carpentieri, G. Finocchio, B. Azzerboni, L. Torres, L. Lopez-Diaz, and E. Martinez, J. Appl. Phys. **97**, 10C713 (2005).
[16] T. Devolder, P. Crozat, C. Chappert, J. Miltat, A. Tulapurkar, Y. Suzuki, and K. Yagami, Phys. Rev. B **71**, 184401 (2005).
[17] J. Miltat, G. Albuquerque, A. Thiaville, and C. Vouille, J. Appl. Phys. **89**, 6982 (2001).
[18] M. J. Donahue (private communication).
[19] A. G. F. Garcia (unpublished).
[20] J. J. Verluijs, M. A. Bari, and J. M. D. Coey, Phys. Rev. B **87**, 026601 (2001).
[21] M. Tsoi, R. E. Fontana, and S. S. P. Parkin, Appl. Phys. Lett. **83**, 2617 (2003).